RECENT SEARCHES FOR NEW PHENOMENA WITH THE ATLAS DETECTOR

William J. Fawcett
University of Cambridge (GB)
william.fawcett@cern.ch

Presented on behalf of the ATLAS Collaboration
DIS2022: XXIX International Workshop on Deep-Inelastic Scattering and Related Subjects
2–6th May 2022, Santiago de Compostela, Spain.

ABSTRACT

Three recently and uniquely interesting searches for new physics performed by the ATLAS collaboration are presented. In each case, innovative search techniques are used to test the Standard Model in new ways. No evidence for new physics is found, but the new techniques developed will open new avenues for further searches in the future.

1 Introduction

The ATLAS Collaboration has produced a wealth of searches for physics beyond the Standard Model (SM). Although no statistically significant deviation from the SM, new and ingenious search strategies continue to be developed. Three new searches from ATLAS that have unusual and interesting search techniques are presented. All searches were performed with an integrated luminosity of 139 fb^{-1} recorded by the ATLAS detector in Run 2 of the LHC. Using the short names of these searches, they are: the pixel dE/dx search (1), the $e\mu$ asymmetry search (2) and the displaced/non-pointing photon search (3).

2 The pixel dE/dx search

Many extensions to the SM, including supersymmetry, predict the existence of new, massive, long-lived particles (LLPs) that have decay lengths long enough to be observed using particle detectors. The hypothetical gluino (the supersymmetric partner of the gluon) has already been tightly constrained by existing LHC searches (4), and so is expected to have a large mass if produced at the LHC. Since these particles are heavy, they will travel with velocities that have fractions of the speed of light, β that are sufficiently less than 1. Furthermore, in the case of the gluino, if it is sufficiently long-lived, it can interact via the strong force with SM particles to form an "R-hadron", which could carry electric charge. This leaves a signature of a heavy, non-relativistic particle that would leave anomalously high ionisation in the ATLAS pixel tracking detector. An excess of events with tracks originating from particles with large mass, compared to the background prediction, would be an indication of new physics, and this search, detailed in Ref (1), exploits that signature. Although this argument has been presented for the gluino, the search was made sufficiently general so that it would be sensitive to any heavy particle beyond the SM (BSM) particle produced with β measurably less than 1.

2.1 Analysis Strategy, Track Mass Determination and Background Estimate

Events were selected using a missing energy trigger, with an offline selection of $E_{\text{T}}^{\text{miss}} > 170\,\text{GeV}$. From these events, a subset of tracks were selected using the following criteria: ensuring that tracks traversed the pixel barrel ($|\eta| < 1.8$), large transverse momentum ($p_{\text{T}} > 120\,\text{GeV}$), isolation, and large ionisation ($\text{d}E/\text{d}x > 1.8\,\text{MeV}\,\text{g}^{-1}\,\text{cm}^2$).

The track mass measurement is briefly described here, and ultimately derives from the ionisation (charge collection) measurements made by the pixel detector as a charged particle travels through it. A charged particle crossing the pixel detector often crosses multiple individual pixels in each layer, and these are joined together to form a cluster. The ionisation measurement ($\text{d}E/\text{d}x$) assigned to each track is the average of the ionisation measurements all clusters

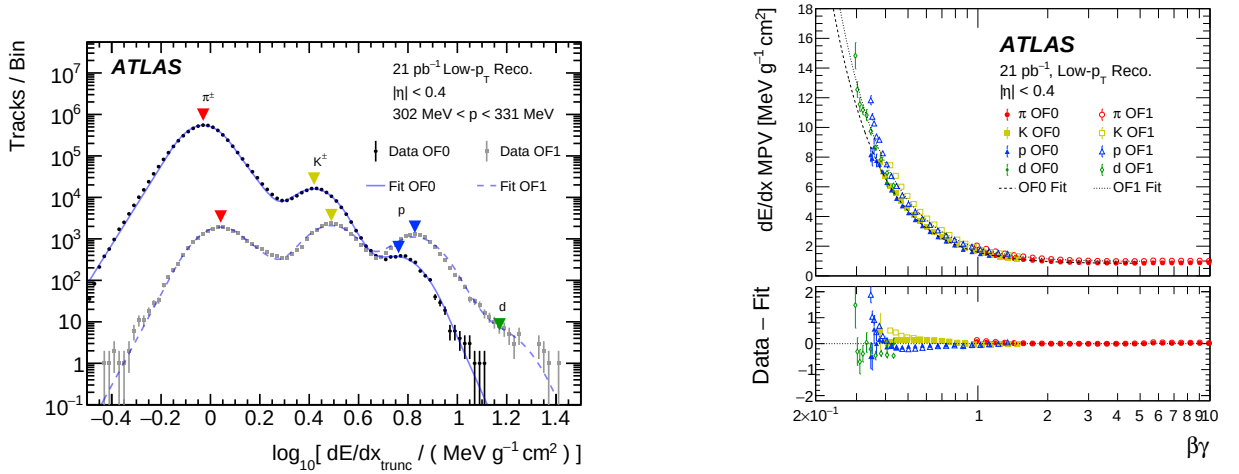

(a) (b)

Figure 1: Distribution of $\langle \mathrm{d}E/\mathrm{d}x \rangle_{\mathrm{trunc}}$, showing distinct particle species (a), and the calibrated fit showing the relationship between $\langle \mathrm{d}E/\mathrm{d}x \rangle_{\mathrm{corr}}$ and $\beta\gamma$ (b). In both (a) and (b) above, data from the special low-pileup run is used, in which the different particle species can be identified. OF0 and OF1 correspond to separate datasets based on IBL (innermost pixel layer) overflow conditions – see Ref (1) for more details. Figures taken from Ref. (1).

belonging to that track. Several corrections are made to the ionisation measurement. The specific ionisation follows a Landau distribution, and to reduce the effects of the tails of this distribution, a truncated average $\langle \mathrm{d}E/\mathrm{d}x \rangle_{\mathrm{trunc}}$ is evaluated after removing the highest $\mathrm{d}E/\mathrm{d}x$ cluster from each track. A second correction is applied to account for the radiation damage suffered by the ATLAS pixel detector during Run 2: with increased integrated luminosity, the charge collection efficiency of the pixel detector decreased. The output of the correction process is referred to as "corrected $\mathrm{d}E/\mathrm{d}x$", $\langle \mathrm{d}E/\mathrm{d}x \rangle_{\mathrm{corr}}$.

A calibration procedure allows $\beta\gamma$ to be extracted from $\langle \mathrm{d}E/\mathrm{d}x \rangle_{\mathrm{corr}}$, where γ is the Lorentz factor. Data from a special low-pileup run of ATLAS were used, where tracks with transverse momentum as low as 100 GeV can be reconstructed and the contribution to the $\mathrm{d}E/\mathrm{d}x$ spectrum for each SM particle species can be seen, as shown in Figure 1a. Fits to this data can be used to extract the most probable SM particle for a given $\langle \mathrm{d}E/\mathrm{d}x \rangle_{\mathrm{trunc}}$ value, and hence $\beta\gamma$ can be extracted with the measured momentum and known particle mass via $\beta\gamma = p/m$, although some extra corrections must be made to the momentum measurement to correct for the efficiency and momentum resolution effects, which can be large for low-momentum tracks, as well as the bias due to tracks with $p_{\mathrm{T}} < 100\,\mathrm{MeV}$ are excluded from the analysis (see Ref (1) for further details). The result of the calibration procedure is shown in Figure 1b, and from the fit to the data, $\beta\gamma$ can be extracted from the measured $\langle \mathrm{d}E/\mathrm{d}x \rangle_{\mathrm{corr}}$, which when combined with the momentum measurement yields the track mass.

The main background contribution comes from SM processes generating high-p_{T} tracks with a large $\mathrm{d}E/\mathrm{d}x$ that is randomly produced according to the Landau distribution of minimum ionising particles. A fully data-driven technique is used to generate the background estimate; and brief details will be given here. The signal region selections are inverted to create two control regions for each signal region, "CR-kin" and "CR-dEdx". Samples are drawn from the $1/p_{\mathrm{T}}$ distribution in CR-kin and combined with samples drawn from the $\mathrm{d}E/\mathrm{d}x$ distribution in CR-dEdx to calculate a track mass distribution. This sampling is performed in bins of $|\eta|$ where η is the pesudorapidity. This distribution is normalised and checked for closure in dedicated validation regions.

2.2 Results

The data are split into 8 signal regions, sub-divided by the $\mathrm{d}E/\mathrm{d}x$ value and whether or not a track is only measured in the ATLAS inner detector (ID) or if it is also combined with information from the muon chambers. In one signal region, "SR-Inclusive_High" (which is inclusive of tracks that are either measured only in the ID or both in the ID and muon detectors, and has $\mathrm{d}E/\mathrm{d}x > 2.4\,\mathrm{MeV\,g^{-1}\,cm^2}$), an excess of data over background was measured with a local significance of 3.6σ and a global significance of 3.3σ. However cross-checks performed after unblinding the data revealed that tracks causing the excess have $\beta \approx 1$ and therefore do not support a heavy LLP signal interpretation. The mass distribution for tracks in SR-Inclusive_High is shown in figure 2a. Since there is no signal-like excess, limits are

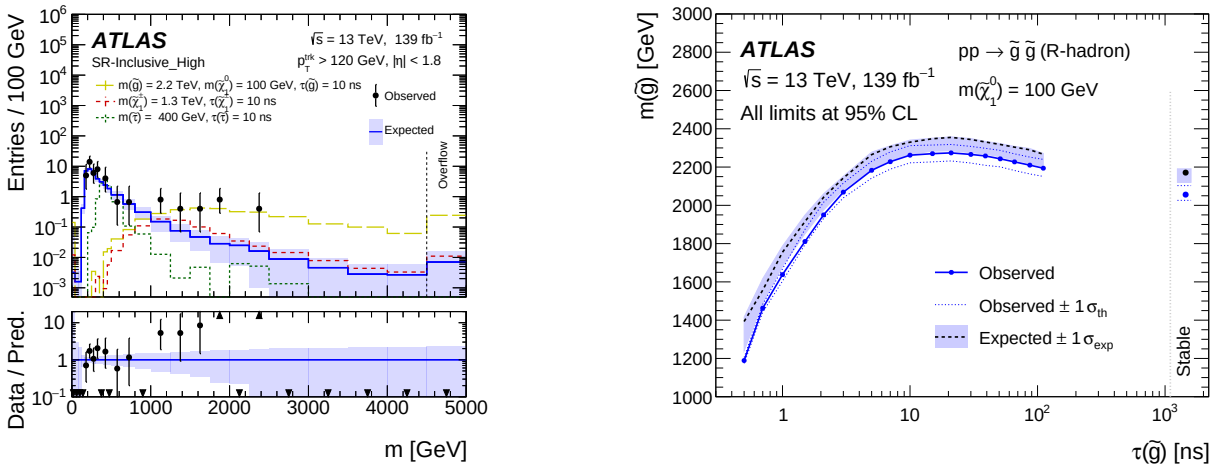

(a) (b)

Figure 2: Distribution of the track mass for data and the background prediction in the "SR-Inclusive_High" signal region (left), and 95% CL limits on the gluino R-hadron model (right).

set on a series of simplified signal models, with the example of a pair-production of gluinos (creating R-hadrons) shown in figure 2b.

3 The $e\mu$ Asymmetry Search

The SM predicts that the ratio

$$\rho = \frac{\sigma(pp \to e^+\mu^- + X)}{\sigma(pp \to e^-\mu^+ + X)} \tag{1}$$

should be approximately unity, if one ignores small lepton-flavour- and CP-violating effects. However, when one considers the effects of the LHC and the ATLAS detector, there are a number of biases that affect this ratio. One example comes from events where a W boson is produced in association with jets, and the W decay produces a muon and neutrino: $W(\to \mu\nu_\mu) + \text{jets}$. If the jet is misidentified as an electron (a "fake" electron) then this process can appear as the $e\mu$ state in an analysis selection. At the LHC, we produce more W^+ bosons than W^- bosons due to the $(pp)^{2+}$ initial state, and as a result, $W+$ jets events can produce more $e^-\mu^+$ events that the CP conjugate, which in turns pushes $\rho \leq 1$. As detailed in Ref. (5), it turns out that almost all biases[1] also favour $\rho \leq 1$. This effect, dubbed the *charge-flavour conspiracy*, gives us an extraordinary gift with which to test the standard model, as any measurement of $\rho > 1$ would be evidence of BSM physics. The first study of this kind by the ATLAS Collaboration is published in Ref (2).

3.1 Example Signal Models

Although there are many possible methods to generate an asymmetry from new physics that would push $\rho > 1$, the analysis concentrated on two concrete examples: an R-parity violating SUSY model, and model with a leptoquark that couples the first and second generations of quarks and leptons.

The R-parity violating SUSY model introduces a non-zero λ'_{231} coupling that couples a down quark, a top quark and a muon, where one of these is exchanged for a superpartner – in this case the muon. When the neutralino is lighter than the top quark, this coupling allows the production of muons in association with top quarks and missing transverse momentum, and in the case that the top quark decays to an electron, yields the $e\mu$ final state. Since the proton's parton distribution for the down quark is significantly larger than for the anti-down, the λ'_{231} coupling would produce significantly more μ^- than μ^+.

[1] With the exception of jet punch-through, which can produce an excess of fake muons when hadrons from jets enter the ATLAS muon chambers. Such events result in what appears to be a "muon jet", with a very large number of muons, and are easily identified and removed during standard event cleaning.

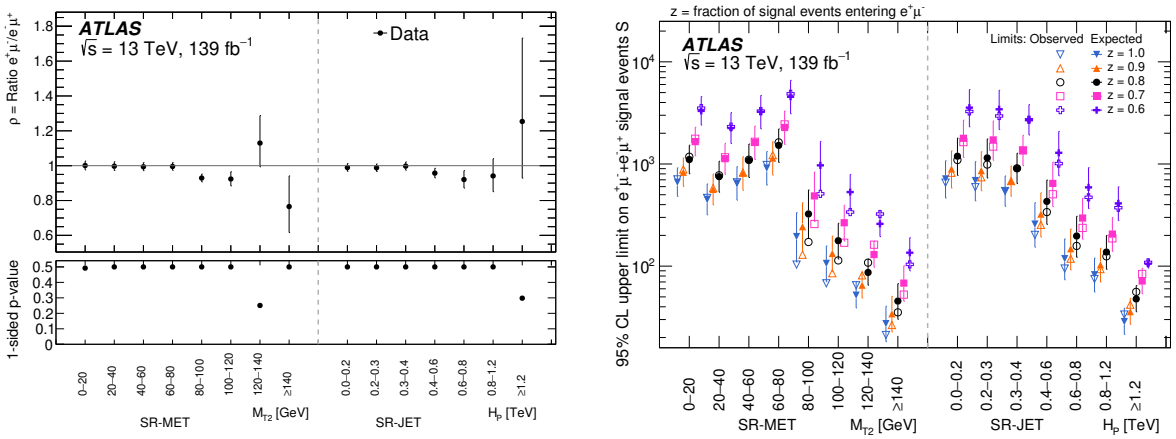

(a) (b)

Figure 3: (a) measured ρ for the general signal regions. (b) observed and expected 95% CL upper limits n the number of signal events entering the $e^+\mu^-$ and $e^-\mu^+$ channels in each bin of SR-MET and SR-JET. The limits are shown for a selection of 'z' values, where z is the fraction of the total number of signal events entering the $e^+\mu^-$ channel. Figures taken from Ref. (2).

The second model introduces a scalar leptoquark, S_1, with couplings permitting $S_1 \to ue^-$ and $S_1 \to c\mu^-$, which can generate an excess of events containing $e^+\mu^-$ over $e^-\mu^+$. For example, consider the tree-level process $ug \to u^* \to S_1, e^+$, with $S_1 \to c\mu^-$. This will dominate over the CP-conjugate process $\bar{u}g \to \bar{u}^* \to \bar{S}_1, e^-$, with $\bar{S}_1 \to \bar{c}\mu^+$, as there the proton's parton distribution for the up quark is significantly larger than for the anti-up quark.

3.2 Analysis Strategy and Results

The analysis strategy was to measure ρ in data, and perform a one-sided test to find if ρ is significantly larger than one. The baseline selection for the analysis is to choose events with exactly one electron and exactly one muon of opposite charge (both with isolation requirements, $|\eta| < 2.47$ and $p_{\mathrm{T}} > 25\,\mathrm{GeV}$), after triggering with $e\mu$ triggers. Since there are no other charge-flavour asymmetry searches, simple selections are preferred over complex ones.

Four signal regions were defined: two generic signal regions, and two that have additional selection requirements designed to target the signal models described in section 3.1. Common to all signal regions is the requirement that $\Sigma(m_{\mathrm{T}}) > 200\,\mathrm{GeV}$, where $\Sigma(m_{\mathrm{T}}) = m_{\mathrm{T}}(e, E_{\mathrm{T}}^{\mathrm{miss}}) + m_{\mathrm{T}}(\mu, E_{\mathrm{T}}^{\mathrm{miss}})$ and m_{T} is the usual transverse mass. The region $\Sigma(m_{\mathrm{T}}) < 200\,\mathrm{GeV}$ is used as a control region. The most general region, SR-MET has no additional selection requirements; the next-most general region, SR-JET has an additionally requires that there be at least one jet. SR-RPV, designed with the R-parity violating SUSY model in mind, is a subset of SR-MET and requires $S > 10$ and $M_{\mathrm{T2}} > 100\,\mathrm{GeV}$, where S is the object-based $E_{\mathrm{T}}^{\mathrm{miss}}$ significance, and M_{T2} is as defined in (6) and built from the electron and muon transverse momenta. Finally, SR-LQ, designed to target the leptoquark model, is a subset of SR-JET, and requires $S > 6$ and the sum of the magnitudes of the transverse momenta of the electron, muon and leading jet to be greater than 1000 GeV.

One of the largest biases comes from fake leptons, and a dedicated data-driven fake estimate was performed to correct for this. Since the presence of fake leptons can push $\rho < 1$, this effect of this bias was estimated and subtracted from the raw data counts for both the $e^+\mu^-$ and $e^-\mu^+$ samples separately before taking the ratio. This enhances the sensitivity to any signal that could push $\rho > 1$. Other biases coming from reconstruction and trigger efficiency differences for positive and negative muons, as well as the muon sagitta bias were corrected for.

The ratio, ρ, is shown for the general signal regions SR-MET and SR-JET in figure 3. These ratios are extracted from likelihood fits to the observed yields in the $e^+\mu^-$ and $e^-\mu^+$ channels, as described in Ref. (2). As there is no significant evidence for $\rho > 1$, limits can be set on the models described in section 3.1, and these are shown in figure 4.

4 The non-pointing/displaced photon analysis

This analysis (3) targets scenarios that generate pairs of photons that do not point towards the primary vertex, and are also displaced in time relative to the bunch crossing of protons in ATLAS. Such signatures could arise from the decays

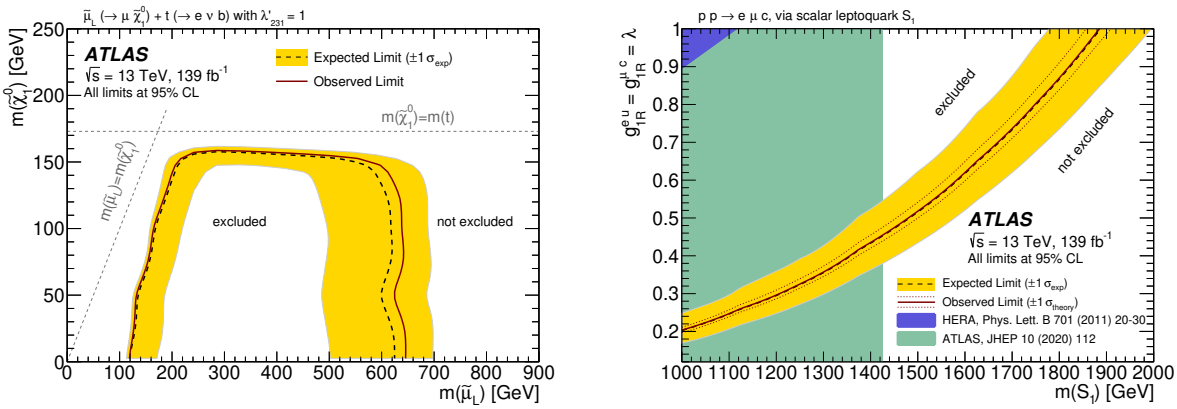

(a) (b)

Figure 4: Expected and observed exclusion limits at 95% CL for the RPV-supersymmetry model (left) and the Leptoquark model (right). Figures taken from Ref. (2).

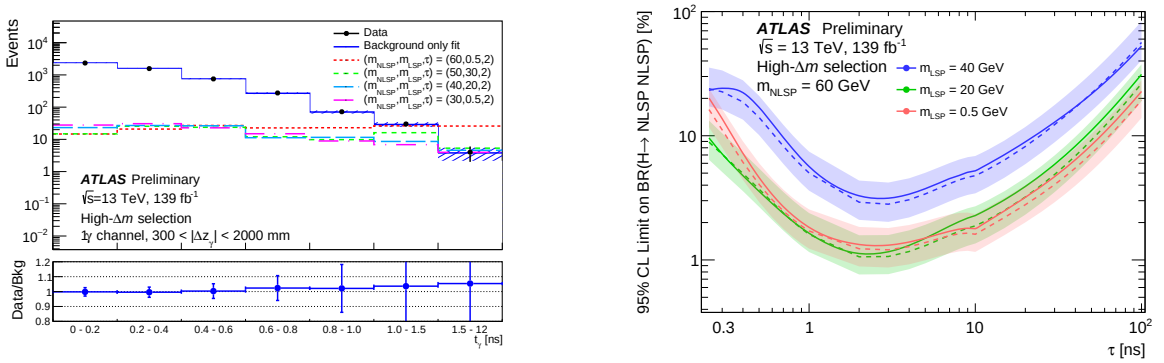

(a) (b)

Figure 5: Data–background comparison for the one-photon signal regions for a variety of photon timings (a), and 95% CL upper limits on the signal model described in the text, for various LSP mass scenarios, as a function of the lifetime of the NLSP (b). Figures taken from Ref. (3).

of neutral long-lived particles (LLPs), for example, a Higgs decay to a pair of LLPs, which each decay to a photon and some other neutral particle. The ATLAS Liquid Argon Calorimeter provides precise pointing and timing information, which is exploited by this search to measure the arrival time and trajectory of photons. Supersymmetry can provide a framework for such a scenario, in particular Gauge Mediated Supersymmetry Breaking models, in which case the Higgs decay chain is denoted $H \to 2 \times \mathrm{NLSP}$, $\mathrm{NLSP} \to \gamma + \mathrm{LSP}$, where (N)LSP stands for (next-to-) Lightest SUSY Particle. Due to the modest Higgs boson mass, the energies of the final state photons, as well as the value of $E_{\mathrm{T}}^{\mathrm{miss}}$, are not sufficiently high to provide a trigger for the events. Instead, the analysis considers SM Higgs boson production in association with either a Z boson, W boson or $t\bar{t}$ system. Leptonic decays of the associated W/Z boson or $t\bar{t}$ system are exploited to provide a single-lepton (electron or muon) trigger.

In addition to the lepton trigger, events are selected with high $E_{\mathrm{T}}^{\mathrm{miss}}$, and two sets of signal regions are defined, one with exactly one photon and another with two or more photons. All photons are required to be displaced in time relative to the bunch crossing, and do not point towards the primary vertex. The signal regions are optimised for different mass splittings between the NLSP and LSP. A data-driven background estimate is performed using control regions with low values of $E_{\mathrm{T}}^{\mathrm{miss}}$, which is validated in a series of non-overlapping validation regions with either intermediate values of $E_{\mathrm{T}}^{\mathrm{miss}}$ or an inverted timing requirement with respect to the signal region.

Figure 5a shows the data–background comparison for the one-photon signal regions, split into bins of different photon timing. No significant excess in the data over the SM background prediction is observed in any of the signal regions, and so limits can be placed on new physics models. Figure 5b show 95% CL upper limits on the branching ratio of $H \to 2 \times \mathrm{NLSP}$ for a variety of photon timing values.

References

[1] ATLAS Collaboration, *Search for heavy, long-lived, charged particles with large ionisation energy loss in pp collisions at $\sqrt{s} = 13$ TeV using the ATLAS experiment and the full Run 2 dataset*, arXiv:2205.06013 [hep-ex]

[2] ATLAS Collaboration, *A search for an unexpected asymmetry in the production of $e^+\mu^-$ and $e^-\mu^+$ pairs in proton-proton collisions recorded by the ATLAS detector at $\sqrt{s} = 13$ TeV*, Phys. Lett. B **830** (2022) 137106.

[3] ATLAS Collaboration, *Search for displaced photons produced in exotic decays of the Higgs boson using 13 TeV pp collisions with the ATLAS detector*, ATLAS-CONF-2022-01

[4] ATLAS Collaboration, *Summary of the ATLAS experiment's sensitivity to supersymmetry after LHC Run 1 – interpreted in the phenomenological MSSM*, JHEP **10** (2015) 134

[5] C. G. Lester and B. H. Brunt, *Difference between two species of emu hides a test for lepton flavour violation*, JHEP **03** (2017) 149.

[6] C. G. Lester and D. J. Summers, *Measuring masses of semiinvisibly decaying particles pair produced at hadron colliders*, Phys. Lett. B **463** (1999) 99.